Quaternary dynamics and plasticity underlie small heat shock protein chaperone function

Florian Stengel[a], Andrew J. Baldwin[b], Alexander J. Painter[a], Nomalie Jaya[c], Eman Basha[c], Lewis E. Kay[b], Elizabeth Vierling[c], Carol V. Robinson[a,1], and Justin L. P. Benesch[a,1]

[a]Department of Chemistry, University of Cambridge, Lensfield Road, Cambridge, CB2 1EW, and Physical and Theoretical Chemistry Laboratory, South Parks Road, Oxford, OX1 3QZ United Kingdom; [b]Departments of Molecular Genetics, Biochemistry, and Chemistry, University of Toronto, Toronto, ON, M5S 1A8, Canada; and [c]Department of Chemistry & Biochemistry, University of Arizona, Tucson, AZ, 85721

Small Heat Shock Proteins (sHSPs) are a diverse family of molecular chaperones that prevent protein aggregation by binding clients destabilized during cellular stress. Here we probe the architecture and dynamics of complexes formed between an oligomeric sHSP and client by employing unique mass spectrometry strategies. We observe over 300 different stoichiometries of interaction, demonstrating that an ensemble of structures underlies the protection these chaperones confer to unfolding clients. This astonishing heterogeneity not only makes the system quite distinct in behavior to ATP-dependent chaperones, but also renders it intractable by conventional structural biology approaches. We find that thermally regulated quaternary dynamics of the sHSP establish and maintain the plasticity of the system. This extends the paradigm that intrinsic dynamics are crucial to protein function to include equilibrium fluctuations in quaternary structure, and suggests they are integral to the sHSPs' role in the cellular protein homeostasis network.

heterogeneity | mass spectrometry | polydispersity | protein dynamics | proteostasis

Small Heat Shock Proteins (sHSPs) are one of the least well understood classes of molecular chaperones, proteins which act to prevent or reverse improper protein associations (1). The importance of the sHSPs is evidenced by their almost ubiquitous expression (2), the presence of multiple sHSP genes in most organisms (3), and their dramatic up-regulation under stress conditions making them among the most abundant of cellular proteins (4). They are implicated in a range of disease states including cataract, cancer, myopathies, motor neuropathies, and neurodegeneration (5–8). The current view of their chaperone action is that they bind unfolding "client" proteins, thereby preventing their irreversible aggregation (9–12). These sHSP:client complexes then interact with ATP-dependent chaperones to allow refolding of the clients (9–12). Structural interrogation of the complexes they form with clients has however been hampered by their apparent heterogeneity, and their organization remains consequently very poorly defined (13–15).

MS is an emergent technology for the structural biology of protein assemblies (16), allowing the interrogation of a wide range of biomolecular systems, including those complicated by polydispersity and dynamics (17, 18). Here we capitalize on these unique advantages to study the complexes formed between pea HSP18.1 and a model client protein, firefly luciferase (Luc). HSP18.1 represents the family of class I cytosolic plant sHSPs which accumulate at heat-shock temperatures (≥38 °C) to ≈1% of the total cellular protein (19). Extensive in vitro studies have established that HSP18.1 is able to bind destabilized clients, enabling subsequent refolding by the HSP70 machinery (20, 21). With the in vivo clients of HSP18.1 yet to be identified, Luc was chosen as it is extremely thermo-sensitive and has been used extensively in chaperone studies (12). Luc does not interact with HSP18.1 at room temperature, even with extended incubation times, but upon heating is protected from precipitation (13, 21). Recent results have shown that the flexible N-terminal region of the HSP18.1 sequence is responsible for binding clients (22), but the quaternary organization of the resulting sHSP:client complexes has remained elusive.

Here we employ a combination of thermo-controlled, time-resolved, and tandem-MS approaches to elucidate molecular details of complex formation. We find that the dodecameric HSP18.1 undergoes both dissociation into suboligomeric species, and expansion into high-order oligomers at heat-shock temperatures. Upon the addition of Luc, large and polydisperse sHSP:client complexes are rapidly formed. We monitor the kinetics of this reaction, and show it to be bimodal, revealing distinct "binding" and "augmentation" phases. Our tandem-MS approach allows us to indentify and quantify the individual complexes which comprise the heterogenous sHSP:client ensembles, uncovering that they are comprised of a variable number of both HSP18.1 and Luc. We observe over 300 different complex stoichiometries, revealing a remarkable diversity of interaction between sHSPs and their clients. It therefore appears that the sHSPs act as an extensive and plastic chaperone ensemble, facilitating their protection of a wide range of clients.

Results

A Transition from Monodisperse Dodecamer to Polydisperse Ensemble Occurs at Heat Shock Temperatures.
To investigate thermally regulated changes in quaternary organization we obtained nanoelectrospray (nES) mass spectra of HSP18.1 at a range of temperatures (Fig. 1A). At 22 °C we observe a single discrete charge state series centered around a 34+ ion at 6,350 m/z, corresponding to a dodecamer of 216,017 Da. This is in accord with our previous analytical ultracentrifugation (20) and MS (23) measurements, as well as the crystal structure of the closely related HSP16.9 from wheat (24). As the temperature of the solution is increased we observe a reduction in signal corresponding to dodecamer, and new signal appearing both below 3,000 m/z and above 7,000 m/z. The former corresponds to populations of monomer and dimer, and the latter to a range of oligomeric sizes, from 13 to 20-mer (Fig. S1). Therefore at elevated temperatures HSP18.1 dodecamers appear to both dissociate into suboligomeric species, and be augmented to form higher-order oligomers.

To interrogate these thermally regulated changes in detail we determined the relative populations of these species and, thereby, the allocation of the constituent subunits amongst the different oligomeric states (Fig. 1B). This demonstrates a clear change in protein partitioning at heat-shock temperatures, with most of the
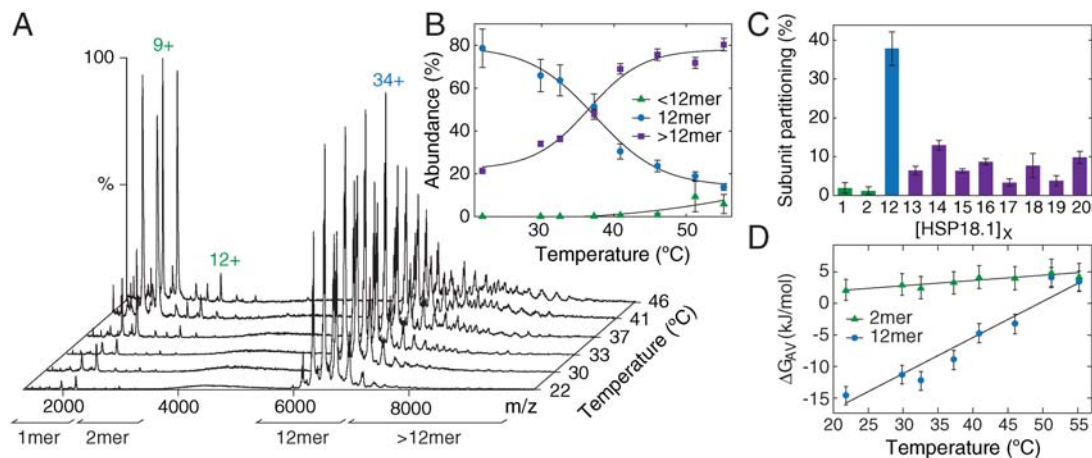
Fig. 1. Temperature-induced changes in HSP18.1 oligomerization. *A* nES mass spectra of HSP18.1 obtained at temperatures from 22 °C to 46 °C. At the lowest temperatures we observe HSP18.1 to exist almost exclusively as a 216 kDa dodecamer, with charge states centered around 6, 350 *m/z* At higher temperatures monomers and dimers are observed at low *m/z*, and higher-order oligomers at high *m/z*, demonstrating the temperature-dependent dissociation and augmentation of the dodecamers. *B* A plot of the relative amount of HSP18.1 subunits existing in different oligomeric states shows that most of the HSP18.1 is redistributed from the dodecamers to high-order oligomers under heat-shock conditions. *C* Close examination of the abundance of the different species at 46 ° C shows a clear preference relative to a Gaussian distribution ($p < 0.01$) for oligomers with an even number of subunits. *D* Plots of the difference in free energy between a subunit free in solution or incorporated into either a dimer or dodecamer follow linear trends, suggesting that neither undergo significant structural change upon thermal activation. In all graphs the data and error bars represent the mean and standard deviation of three independent experiments.

protein being reallocated from dodecamers into higher-order oligomers. Quantification of the number of monomers populating the different higher-order oligomeric states shows that those composed of an even number of subunits are clearly favored over those with an odd number (Fig. 1*C*). The resulting "saw-tooth" distribution, along with the increasing presence of free monomers and dimers at heat-shock temperatures, suggests that higher-order oligomers result from the dissociation of dodecamers into suboligomeric species, which subsequently recombine with oligomeric species. Such a mechanism for oligomeric rearrangement is consistent with the rate-limiting step in HSP18.1 subunit exchange being dissociation of the dodecamer (23), and, through the increased amount of suboligomeric species at elevated temperatures, provides a rationale for the temperature-dependence of subunit exchange (13, 25). These thermal rearrangements in quaternary organization are reversible (Fig. S2). Interestingly, the polydisperse and saw-toothed distribution we observe is very similar to the distribution of oligomers populated by the mammalian sHSPs αA- and αB-crystallin at ambient conditions (26), raising the possibility that a polydisperse ensemble of oligomers may be a widespread feature of functional sHSPs.

Thermally Induced Changes Are Underpinned by Quaternary Protein Dynamics. To extract thermodynamic parameters for these thermal rearrangements we considered the equilibrium of a single protein subunit between its free state in solution, and its bound state within an oligomer. As such we can define an equilibrium constant, and hence an average subunit free energy (ΔG_{AV}, *Supporting Information Methods*). The free energies are found to scale linearly with temperature, allowing elucidation of the enthalpic and entropic components to the free energy (Fig. 1*D*, Fig. S3). For the dodecamer these values were determined as $\Delta H_{AV} = -184 \pm 12$ kJmol^{-1} and $\Delta S_{AV} = -570 \pm 40$ Jmol^{-1}, and for the dimer $\Delta H_{AV} = -22 \pm 2$ kJmol^{-1} and $\Delta S_{AV} = -84 \pm 7$ Jmol^{-1}. The linear scaling of free energy with temperature shows that the temperature dependence of the oligomer distributions can be explained simply by the interplay of the stabilities of a single set of structures, and that it is unnecessary to propose that the individual oligomers themselves undergo large structural rearrangements at heat-shock temperatures. This surprising result is contrary to what has been observed for HSP26 from yeast, in which a conformational change of its "middle domain" underlies

the thermal activation of its chaperone function (27). The presence of such a middle domain however appears unique to HSP26 (27), and is certainly absent in HSP18.1 (12). Our results here indicate that, at least for HSP18.1, activation is mediated not by an alteration in secondary or tertiary structure, but rather a dynamical change in quaternary organization that results from the varying thermodynamic stabilities of the individual sHSP oligomers.

Protection of Client Occurs Through the Bimodal Formation of an Ensemble of Polydisperse Complexes. To examine its chaperone function, we obtained MS spectra of HSP18.1 incubated at 42 ° C for varying times with the model client Luc, at a 1 : 1 molar ratio of HSP18.1 (dodecamer) and Luc (monomer) (Fig. 2*A*). Before heating, major charge state envelopes are observed around 4,000 and 6,500 *m/z*, corresponding to unbound Luc monomer and HSP18.1 dodecamer respectively. After as little as 30 s of incubation the concentration of free Luc decreases, and concomitantly a broad and largely unresolved area of signal is observed above 8,000 *m/z*, indicating the formation of sHSP:client complexes. This signal increases with longer incubation and also shifts to higher *m/z*, showing that not only are more complexes formed but also that they become more massive.

By quantifying the relative abundances of these different species, we can extract their rates of disappearance or formation (Fig. 2*B*). We find that the decay of Luc is fitted by a single exponential, giving a rate constant of 2.41 ± 0.32 min^{-1}. The formation of complex however is fitted by a biexponential, with an initial fast phase (2.27 ± 0.13 min^{-1}) and a subsequent slow phase (0.11 ± 0.03 min^{-1}), which is mirrored by the decay of HSP18.1 dodecamer. From the mean *m/z* of signal corresponding to complex we can estimate a mean mass (Fig. S4), and we find that this also follows biexponential kinetics, with rate constants of 1.83 min^{-1} and 0.05 min^{-1}. Together, this demonstrates that sHSP:client complex formation has two distinct stages, an initial binding phase, in which client is bound and aggregation prevented, and a subsequent augmentation phase. This second stage involves the incorporation of additional sHSP, presumably to reach optimal stability of the complex.

Tandem Mass Spectrometry Allows the Deconvolution of the Polydisperse Ensemble of Chaperone:Client Complexes. The signal at high *m/z* is characteristic of a polydisperse ensemble, the many
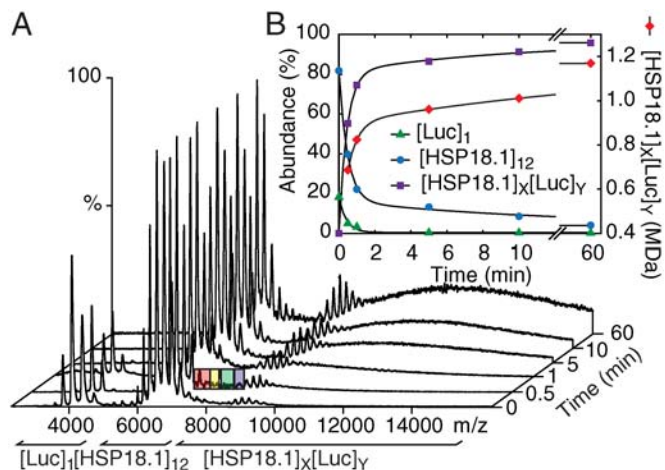
Fig. 2. Time-course of the formation of complexes between HSP18.1 and unfolding Luc. *A* Incubation with HSP18.1 ($\approx 6,350$ *m/z*) at 42 °C results in a decrease in the abundance of Luc ($\approx 4,100$ *m/z*), and the concomitant appearance of signal at high *m/z* (>8,000 *m/z*) corresponding to sHSP:client complexes. Data are normalised such that the HSP18.1 is displayed at an intensity of 100%. Coloured boxes refer to isolations for tandem-MS experiments in Figure 4. *B* Quantifying the relative abundances of the different species shows the initial rapid binding of Luc by HSP18.1, followed by further incorporation of HSP18.1 into the resultant complexes. The average mass of these complexes (*Red*, right-hand *y*-axis) mirrors this behavior, revealing the presence of distinct "binding" and "augmentation" steps in the chaperone action of HSP18.1.

components of which give rise to extensive peak overlap, frustrating attempts at spectral interpretation. We have previously developed a tandem-MS methodology to allow the interrogation of heterogeneous systems (28). We first examined a 1:0.1 mixture of HSP18.1 and Luc which had been incubated at 42 °C for 10 min, with the resulting complexes separated from the remaining HSP18.1 by size exclusion chromatography (SEC) (Fig. S5). We chose this ratio to ensure complete protection of Luc while keeping the entire range of complexes amenable for MS interrogation. An MS spectrum of the resulting complexes displays a broad area of signal from 8,000 to 13,000 *m/z* (Fig. 3*A*). Ions comprising the most intense complex peak, at 8,950 *m/z*, were

selected and activated by energetic collisions with argon atoms, resulting in the appearance of signal at both low and high *m/z* (Fig. 3*B*). The former corresponds to HSP18.1 monomers, and the latter to species having been stripped of one (10,000–16,800 *m/z*) or two monomers (19,000–30,000 *m/z*) (Fig. S6). This asymmetric dissociation of the oligomers is a general feature for activated protein complexes in the gas phase (29), and leads to an effective charge reduction of the species being interrogated (30). The resulting increased separation between charge states is such that masses can be measured that are accurate enough to determine unambiguously the stoichiometries of the sHSP:client complexes (Fig. S7). Assignment and relative quantification of the different species reveals, for this isolation, a polydisperse ensemble of HSP18.1 binding one Luc client (Fig. 3*C*). Analogous tandem-MS experiments were performed on the different peaks in the MS spectrum corresponding to HSP18.1:Luc complex (Fig. S8), and results combined to provide a comprehensive view of the oligomers comprising the polydisperse ensemble. At this ratio we identified complexes containing one Luc and as few as 14, or as many as 25, HSP18.1 subunits. Furthermore, we find that complexes with an even number of sHSP subunits bound to a client are more abundant than those with an odd number. This mirrors the saw-tooth pattern observed for HSP18.1 at elevated temperatures in the absence of client (Fig. 1*C*). This strongly suggests that the dissociation of dodecamers and formation of higher-order oligomers, via thermally regulated quaternary dynamics, constitutes a molecular activation integral to the chaperone function of HSP18.1.

Dimers and Monomers Mediate Different Stages of Complex Formation. To examine the initial stages of complex formation we performed similar tandem-MS experiments after only 30 s of incubation, at a 1:1 ratio (Fig. 4*A*). We selected regions at low *m/z*, corresponding to small, and hence early, complexes for dissociation. In this series of experiments we observe a number of different higher-order sHSP oligomer and sHSP:client complex stoichiometries. The presence of both these two classes of species, as well as unbound Luc and HSP18.1 dodecamer, confirms that these conditions allow us to examine the early phase of complex formation. Notably, despite tandem-MS interrogation of the entire region in the mass spectrum where a hypothetical $[\text{HSP8.1}]_{12}[\text{Luc}]_1$ complex would appear (7,000–8,500 *m/z*,
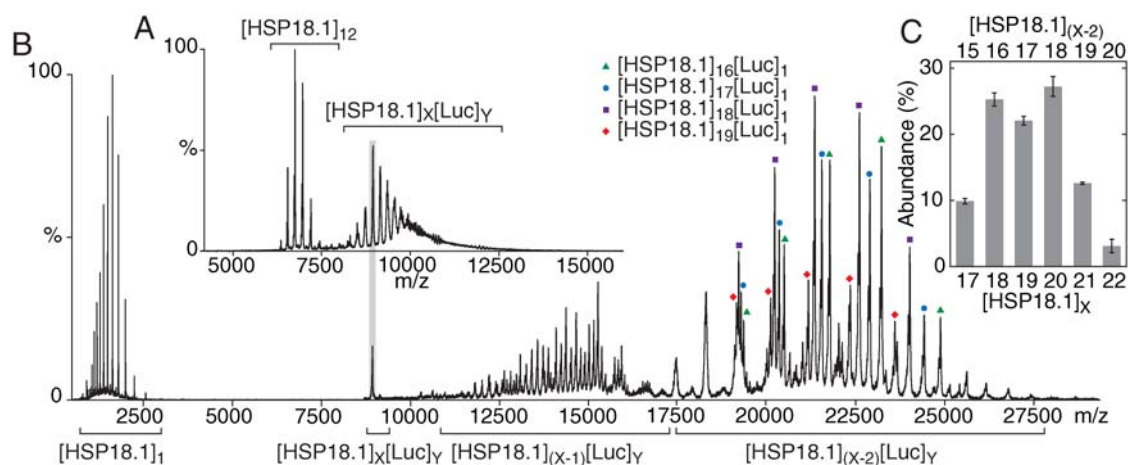

Fig. 3. Identification and quantification of HSP18.1:Luc complexes by means of tandem-MS. *A* Spectrum of a complex formed between HSP18.1 and Luc at a 1:0.1 ratio. Unbound dodecamer is observed around 6,350 *m/z*, and a broad area of signal, characteristic of a polydisperse ensemble, is observed above 8,000 *m/z*. *B* Selection of ions at a particular *m/z*, gray, and activation of selected ions leads to the removal of highly charged HSP18.1 subunits ($\approx 1,800$ *m/z*) from the parent oligomers. Complementary stripped complexes appear at high *m/z*, sufficiently separated that they can be assigned unambiguously (Fig. S6). *C* Relative quantification of the different complexes from the heights of the peaks reveals a number of different stoichiometries of HSP18.1 bound to one Luc, and a dominance ($p < 0.01$) of those containing an even number of HSP18.1 subunits relative to a Gaussian distribution. This saw-tooth pattern mirrors that observed when HSP18.1 is heated on its own, (Fig. 1*C*), revealing the importance of temperature controlled dynamics of the sHSP in complex formation. Data and error bars represent the mean and standard deviation of three experiments.
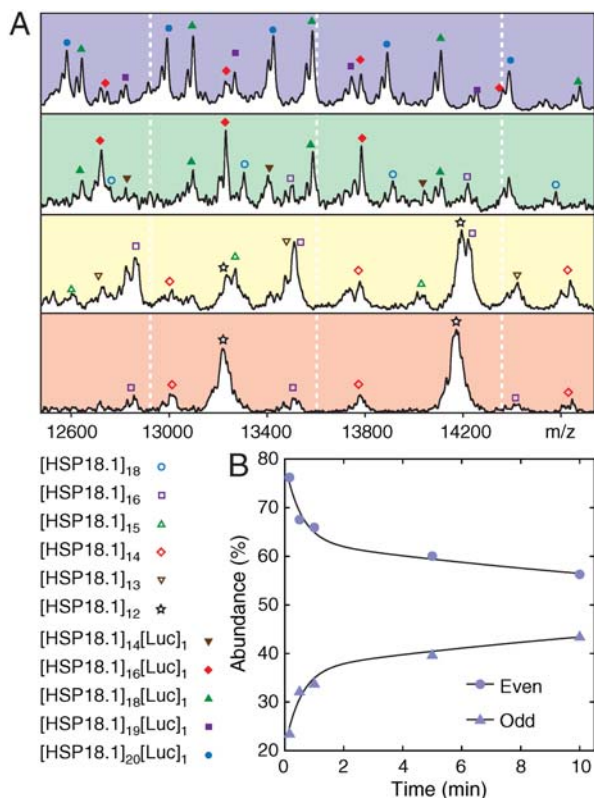
Fig. 4. Population of oligomers during the formation of HSP18.1:Luc complexes. *A* Analogous tandem-MS experiments to that in Fig. 3*B* performed for different isolations (c.f. Fig. 2*B*) of a 30 s incubation of HSP18.1 and Luc, at a 1:1 ratio. An expansion of the $[HSP18.1]_{(X-1)}[Luc]_Y$ region is shown. A range of complexes and higher-order oligomers are identified, with the labelling referring to the parent oligomer. Theoretical peak positions arising from dissociation of $[HSP18.1]_{12}[Luc]_1$ are indicated by dashed white lines, and do not correspond to the charge state series observed. This suggests this species is not formed during protection of Luc. *B* Quantifying the stripped oligomers shows that the abundance of complexes with an even number of subunits is higher than those with an odd number at all timepoints. However this difference is greatest at earlier time points. Overlaying the parameters determined in Fig. 2*B* for the binding and augmentation steps in complex formation gives an excellent fit, suggesting that dimers are involved in the client binding process.

Fig. S4), we find no evidence for this species. Though qualified by our limit-of-detection (5% of the most abundant peak in a single tandem-MS spectrum), this suggests that the HSP18.1

dodecamer is not directly involved in substrate binding. Instead, it seems the role of the dodecamer is as a reservoir of HSP18.1 subunits which can then set up the polydisperse ensemble for substrate binding.

We performed additional tandem-MS experiments at 8,250 m/z, as in the top panel of Fig. 4*A*, but at different incubation times. From quantifying the abundance of the resulting complexes it is apparent that at the complexes with an even number of HSP18.1 subunits are more abundant than those with an odd number. Moreover, this disparity is largest at the earliest time points (Fig. 4*B*). Plotting the relative abundance of these "even" complexes versus the "odd" ones, and applying the biexponential parameters resulting from the binding and augmentation phases (from Fig. 2*B*), gives an excellent fit. Taking this together with our previous observation that the HSP18.1 dodecamer undergoes a rapid exchange of subunits, with dimers exchanging faster than monomers (23), strongly suggests that dimers play a crucial role in initial complex formation, and that the slower rearrangements to achieve optimal stability are additionally mediated by the movement of monomers.

The Polydisperse Ensemble of Complexes Contains Variable Numbers of Both Chaperone and Client. To examine the full distribution of complexes formed at this 1:1 sHSP:client ratio we performed similar experiments on a fraction (11.5–12.3 mL) isolated by SEC (Fig. 5*A*). Remarkably we are able to identify unambiguously and quantify species containing 14 to 36 HSP18.1 subunits, and 1 to 3 Luc (Fig. 5*B*). Furthermore, analogous experiments performed with another client protein, citrate synthase, reveal a similar range of binding stoichiometries (Fig. S9). Therefore we can deduce that sHSP:client complexes can contain a variable number of both chaperone and client components.

By convoluting these tandem-MS-derived distributions for this SEC fraction with the whole SEC peak (Fig. S10) we extrapolated the complete distribution of complexes formed at this particular sHSP:client ratio (Fig. 5*C*). The range of complexes formed is striking in its heterogeneity. We observe over 300 different HSP18.1:Luc combinations being populated to greater than 1% of the population of $[HSP18.1]_{24}[Luc]_2$, the most abundant complex under these conditions (Fig. 5*C*). This reveals why characterization of the complexes formed between sHSPs and clients has proven elusive by using traditional structural biology approaches, and highlights the utility of MS for studying polydisperse protein ensembles. Moreover, while ATP-dependent molecular chaperones have strict ratios of interaction with their clients (31–33), the picture that emerges here for the ATP-inde-
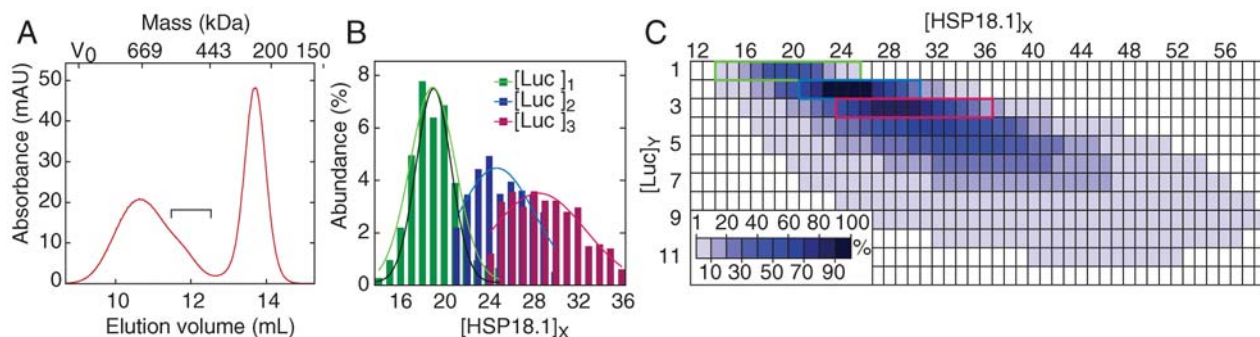

Fig. 5. HSP18.1 forms a remarkably disperse range of complexes with Luc *A* Size exclusion chromatogram of a 1:1 incubation of HSP18.1 and Luc, showing a peak at long elution times corresponding to HSP18.1 dodecamer, and a broad peak at shorter elution times corresponding to complexes between sHSP and client (see also Fig. S4). A fraction corresponding to the low-mass end of the complexes, bracketed, was chosen for MS analysis. *B* Histograms and fits for the abundance of the different complexes for the fraction determined from tandem-MS experiments. Overlaid is the fit to the distribution obtained in Fig. 3*C* (*Black*). Complexes are composed of a variable number of both sHSP and client. *C* Extrapolating the tandem-MS-derived distributions according to the SEC data reveals the distribution of all HSP18.1:Luc complexes formed at a 1:1 incubation. Experimentally identified complexes are ringed. Over 300 complexes of over 1% relative intensity are thus observed, revealing a remarkable heterogeneity in the stoichiometries of interaction between sHSPs and clients.

pendent sHSPs is the complete inverse: they appear defined by the diversity of their interaction.

Discussion

The Chaperone Action of HSP18.1 is Regulated by Quaternary Protein Dynamics. Here we have found that HSP18.1 exists as a dodecameric oligomer in equilibrium with dimers, monomers, and higher-order oligomers (Fig. 6*A*). At elevated temperatures, where HSP18.1 performs its protective role, these equilibria shift such that the majority of the protein is partitioned to these higher-order oligomeric states. Upon the addition of unfolding client, complexes are formed, holding the client stable relative to precipitation (Fig. 6*A*). Notably multiple higher-order oligomer states are observed, and the complexes are remarkable in their polydispersity, varying in both the number of both sHSP and client subunits. This is surprising considering HSP18.1 exists as a monodisperse dodecamer at ambient conditions. Moreover, considering that no complexes are observed containing 12 or fewer HSP18.1 subunits, this strongly indicates that the dodecamer is not directly involved in the binding of client protein. Rather it appears that the dodecamer exists as a reservoir for suboligomeric species which are released under heat-shock conditions, and can assemble with residual oligomers to form higher-order oligomers. This thermally activated dynamical change in oligomerisation thereby produces the active chaperoning ensemble of the sHSP. Stress-regulated switching between multiple functions, with higher-order oligomers displaying ATP-independent
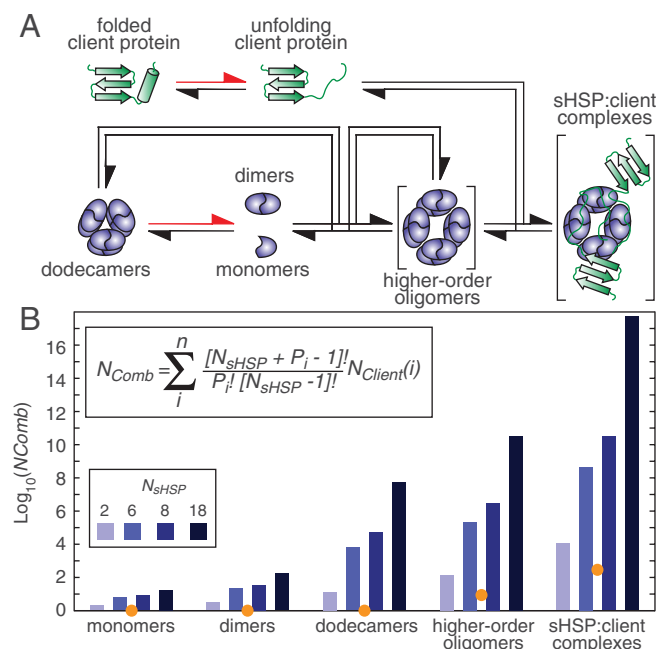

Fig. 6. sHSPs establish a disperse chaperone network. *A* The dodecameric form of HSP18.1 represents a "storage" form, which is in equilibrium with suboligomeric species, and, through recombination with these, higher-order oligomers. These higher-order species are themselves continually recycling through the loss and reincorporation of dimers and monomers. Upon heat-shock the equilibria shift (*Red*) from the dodecamer to dissociated species, and unfolding clients are bound to form sHSP:client complexes. *B* From the number of different species we observe here for the different states of HSP18.1 (*Orange*) we can extrapolate to systems incorporating multiple sHSPs (*Bars*). Based on the ability of related sHSPs to hetero-oligomerise, the number of potential species (N_{Comb}) can be calculated using the inset equation, where N_{sHSP} is the number of compatible sHSPs, *i* the number of HSP18.1 subunits in the oligomer, and N_{Client} the number of different bound states for a particular *i*. This reveals a remarkably extensive potential sHSP network, presumably catering for the array of different unfolding clients requiring protection from aggregation during cellular stress.

chaperone activity, has been observed for enzymes in yeast (34) and Arabidopsis (35). It may be that the dodecameric form of HSP18.1 is chaperone-inactive simply to prevent unproductive associations with protein chains under recovery conditions. In light of the multiple functions of the α-crystallins (36, 37), vertebrate members of the sHSP family, the fascinating possibility that HSP18.1 performs a cellular role additional to its chaperone function should not be discounted.

We have shown here that it is these quaternary dynamics which are the molecular basis of HSP18.1 chaperone function. Moreover, rather than relying on ATP, posttranslational modification, or large structural changes, these dynamics are temperature controlled. The importance of intrinsic dynamic fluctuations in secondary and tertiary structure for protein function has become established in recent years (38–40), a paradigm that is extended to the quaternary level by the dynamic regulation of chaperone function described here.

Polydispersity and Subunit Exchange Establish an Extensive and Plastic sHSP Chaperone Ensemble. We have identified over 300 different stoichiometries of interaction between HSP18.1 and Luc, all stemming from a single "parent" form, the dodecamer. This switch from monodisperse to polydisperse at heat-shock temperatures effectively establishes an ensemble of chaperones. In addition, another consequence of the dynamic quaternary structure of sHSPs is the formation of heterooligomers by coassembly of monomers immediately after their biosynthesis, forming an equilibrium of species maintained via subunit exchange (23–25). In pea another dodecameric cytosolic sHSP, HSP17.9, has been identified which is of the same evolutionary class (19), and hence capable of forming hetero-oligomers with HSP18.1. The pea genome remains incompletely sequenced, but it is likely that more sHSPs compatible with HSP18.1 remain to be discovered, as the number of equivalent sHSPs (N_{sHSP}) in Arabidopsis ($N_{sHSP} = 6$), rice ($N_{sHSP} = 8$), and Californian poplar ($N_{sHSP} = 18$) are considerably greater (41). Using these numbers, we can determine the maximum number of possible combinations of hetero-oligomers (N_{Comb}) for the different organizational states of HSP18.1 we have observed here (Fig. 6*B*).

N_{Comb} scales exponentially with N_{sHSP} such that, based on the complexes seen here for HSP18.1, if $N_{sHSP} = 18$ over 10^{17} combinations are possible! Though factors such as tissue-specific expression levels need to be considered, this provides a glimpse of a remarkably disperse sHSP chaperone ensemble. This is reminiscent of the immune system in higher eukaryotes, whereby a relatively small number of genes (approximately 300) can give rise to over 10^8 different antibodies, allowing the recognition of the diverse structures of antigens (42). Plants are particularly prone to quotidian cycles of heat stress, and the resulting protein aggregation represents a major insult to maintenance of cellular protein homeostasis, or proteostasis (43). It is tempting to speculate that evolution of such an extensive sHSP ensemble, within the context of the wider chaperone network, allows plants to protect themselves against the diversity of unfolding client proteins, thereby maintaining proteostasis.

Materials and Methods

Mass Spectrometry. Mass spectra were obtained on an liquid chromatography time-of-flight (LCT) or quadrupole time-of-flight (Q-ToF) 2 (both Waters) according to a previously described protocol (44). A custom-built nES probe was employed for the spectra of HSP18.1 at different temperatures as described previously (45). In all cases the buffer was 200 mM ammonium acetate, pH 6.8.

The following instrument parameters were used on the LCT: nES capillary 1.6 kV, sample cone 160 V, extractor cone 40 V, ion transfer stage pressure 9.3 mbar and 2.1×10^{-6} mbar ToF analyser pressure. The following parameters were used on the Q-ToF 2: nES capillary 1.6 kV, sample cone 160 V, extractor cone 40 V, accelerating voltage into the collision cell 30 V, ion transfer stage pressure 9.6×10^{-3} mbar, quadrupole analyser pressure

1.0×10^{-5} mbar, and ToF analyser pressure 8.1×10^{-6} mbar, with the collision cell pressurised to 35 μbar (argon). For tandem-MS the accelerating voltage was raised up to 200 V.

Proteins. HSP18.1 from *Pisum sativum* was expressed in *E. coli* and purified as described previously (20). Recombinant luciferase from *Photinus pyralis* was purchased from Promega (Catalog E1701). Samples were buffer-exchanged using SEC at 6 °C (Superdex 200 HR10/30, GE Healthcare) or centrifugal concentrators (Vivaspin, Sartorius), and adjusted to the desired concentration using theoretical (46) extinction coefficients of 198,000 (HSP18.1 dodecamer) and 39,810 (Luc monomer).

To form complexes, HSP18.1 was incubated with Luc at 42 °C in a water bath for the desired time. The reaction was quenched on ice, which arrests complex formation but does not cause complex disassembly (13). Complexes were either formed in 200 mM ammonium acetate (pH6.8), or buffer A (150 mM KCl, 5 mM MgCl, 2 mM Hepes, 2 mM DTT, pH7.5) as stated in the text. For the experiments assessing the kinetics of complex formation (Fig. 2), the concentrations of HSP18.1 (dodecamer) and Luc (monomer) were both 2 μM. For tandem-MS analysis (Fig. 3), complexes were prepared in buffer A using 12 μM HSP18.1, and isolated by SEC. The chosen fractions were then concentrated to ~2 μM complex for tandem-MS analysis.

Quantitative and Thermodynamic Analysis of HSP18.1. The relative abundances of the different oligomers in a particular spectrum were obtained from the respective peak heights, an effective means for assessing the populations of species comprising polydisperse ensembles (28), and corrected for the *m/z* dependence of detector efficiency (47). From these abundances we calculated a stability constant and free energy difference between a subunit in its free and bound state (see *Supporting Information Methods*).

1. Ellis J (1987) Proteins as molecular chaperones. *Nature*, 328:378–379.
2. Kappé G, Leunissen JA, de Jong WW (2002) Evolution and diversity of prokaryotic small heat shock proteins. *Prog Mol Subcell Biol*, 28:1–17.
3. Kappé G, et al. (2003) The human genome encodes 10 α-crystallin-related small heat shock proteins: HspB1-10. *Cell Stress Chaperon*, 8:53–61.
4. Malmström J, et al. (2009) Proteome-wide cellular protein concentrations of the human pathogen *Leptospira interrogans*. *Nature*, 460:762–766.
5. Benndorf R, Welsh MJ (2004) Shocking degeneration. *Nat Genet*, 36:547–548.
6. Clark JI, Muchowski PJ (2000) Small heat-shock proteins and their potential role in human disease. *Curr Opin Struct Biol*, 10:52–59.
7. Quinlan R, Van Den Ijssel P (1999) Fatal attraction: When chaperone turns harlot. *Nat Med*, 5:25–26.
8. Sun Y, MacRae TH (2005) The small heat shock proteins and their role in human disease. *FEBS J*, 272:2613–2627.
9. Haslbeck M, Franzmann T, Weinfurtner D, Buchner J (2005) Some like it hot: The structure and function of small heat-shock proteins. *Nat Struct Mol Biol*, 12:842–846.
10. McHaourab HS, Godar JA, Stewart PL (2009) Structure and mechanism of protein stability sensors: Chaperone activity of small heat shock proteins. *Biochemistry*, 48:3828–3837.
11. Narberhaus F (2002) α-crystallin-type heat shock proteins: Socializing minichaperones in the context of a multichaperone network. *Microbiol Mol Biol R*, 66:64–93 table of contents.
12. van Montfort R, Slingsby C, Vierling E (2002) Structure and function of the small heat shock protein/α-crystallin family of molecular chaperones. *Adv Protein Chem*, 59:105–156.
13. Friedrich KL, Giese KC, Buan NR, Vierling E (2004) Interactions between small heat shock protein subunits and substrate in small heat shock protein-substrate complexes. *J Biol Chem*, 279:1080–1089.
14. Haley DA, Bova MP, Huang QL, McHaourab HS, Stewart PL (2000) Small heat-shock protein structures reveal a continuum from symmetric to variable assemblies. *J Mol Biol*, 298:261–272.
15. Stromer T, Ehrnsperger M, Gaestel M, Buchner J (2003) Analysis of the interaction of small heat shock proteins with unfolding proteins. *J Biol Chem*, 278:18015–18021.
16. Benesch JLP, Ruotolo BT, Simmons DA, Robinson CV (2007) Protein complexes in the gas phase: Technology for structural genomics and proteomics. *Chem Rev*, 107:3544–3567.
17. Heck AJ (2008) Native mass spectrometry: A bridge between interactomics and structural biology. *Nat Methods*, 5:927–933.
18. Sharon M, Robinson CV (2007) The role of mass spectrometry in structure elucidation of dynamic protein complexes. *Annu Rev Biochem*, 76:167–193.
19. DeRocher AE, Helm KW, Lauzon LM, Vierling E (1991) Expression of a conserved family of cytoplasmic low molecular weight heat shock proteins during heat stress and recovery. *Plant Physiol*, 96:1038–1047.
20. Lee GJ, Pokala N, Vierling E (1995) Structure and in vitro molecular chaperone activity of cytosolic small heat shock proteins from pea. *J Biol Chem*, 270:10432–10438.
21. Lee GJ, Roseman AM, Saibil HR, Vierling E (1997) A small heat shock protein stably binds heat-denatured model substrates and can maintain a substrate in a folding-competent state. *EMBO J*, 16:659–671.
22. Jaya N, Garcia V, Vierling E (2009) Substrate binding site flexibility of the small heat shock protein molecular chaperones. *Proc Natl Acad Sci USA*, 106:15604–15609.
23. Sobott F, Benesch JLP, Vierling E, Robinson CV (2002) Subunit exchange of multimeric protein complexes. Real-time monitoring of subunit exchange between small heat shock proteins by using electrospray mass spectrometry. *J Biol Chem*, 277:38921–38929.
24. van Montfort RL, Basha E, Friedrich KL, Slingsby C, Vierling E (2001) Crystal structure and assembly of a eukaryotic small heat shock protein. *Nat Struct Biol*, 8:1025–1030.
25. Painter AJ, et al. (2008) Real-time monitoring of protein complexes reveals their quaternary organization and dynamics. *Chem Biol*, 15:246–253.
26. Benesch JLP, Ayoub M, Robinson CV, Aquilina JA (2008) Small heat shock protein activity is regulated by variable oligomeric substructure. *J Biol Chem*, 283:28513–28517.
27. Franzmann TM, Menhorn P, Walter S, Buchner J (2008) Activation of the chaperone Hsp26 is controlled by the rearrangement of its thermosensor domain. *Mol Cell*, 29:207–216.
28. Aquilina JA, Benesch JLP, Bateman OA, Slingsby C, Robinson CV (2003) Polydispersity of a mammalian chaperone: Mass spectrometry reveals the population of oligomers in αB-crystallin. *Proc Natl Acad Sci USA*, 100:10611–10616.
29. Benesch JLP (2009) Collisional activation of protein complexes: Picking up the pieces. *J Am Soc Mass Spectrom*, 20:341–348.
30. Benesch JLP, Aquilina JA, Ruotolo BT, Sobott F, Robinson CV (2006) Tandem mass spectrometry reveals the quaternary organization of macromolecular assemblies. *Chem Biol*, 13:597–605.
31. Bukau B, Weissman J, Horwich A (2006) Molecular chaperones and protein quality control. *Cell*, 125:443–451.
32. Saibil HR (2008) Chaperone machines in action. *Curr Opin Struct Biol*, 18:35–42.
33. Young JC, Agashe VR, Siegers K, Hartl FU (2004) Pathways of chaperone-mediated protein folding in the cytosol. *Nat Rev Mol Cell Biol*, 5:781–791.
34. Jang HH, et al. (2004) Two enzymes in one; two yeast peroxiredoxins display oxidative stress-dependent switching from a peroxidase to a molecular chaperone function. *Cell*, 117:625–635.
35. Lee JR, et al. (2009) Heat-shock dependent oligomeric status alters the function of a plant-specific thioredoxin-like protein, AtTDX. *Proc Natl Acad Sci U S A*, 106:5978–5983.
36. Horwitz J (1992) α-crystallin can function as a molecular chaperone. *Proc Natl Acad Sci U S A*, 89:10449–10453.
37. Piatigorsky J, Wistow G (1991) The recruitment of crystallins: New functions precede gene duplication. *Science*, 252:1078–1079.
38. Henzler-Wildman K, Kern D (2007) Dynamic personalities of proteins. *Nature*, 450:964–972.
39. Smock RG, Gierasch LM (2009) Sending signals dynamically. *Science*, 324:198–203.
40. Vendruscolo M, Dobson CM (2006) Structural biology. Dynamic visions of enzymatic reactions. *Science*, 313:1586–1587.
41. Waters ER, Aevermann BD, Sanders-Reed Z (2008) Comparative analysis of the small heat shock proteins in three angiosperm genomes identifies new subfamilies and reveals diverse evolutionary patterns. *Cell Stress Chaperon*, 13:127–142.
42. Tonegawa S (1983) Somatic generation of antibody diversity. *Nature*, 302:575–581.
43. Balch WE, Morimoto RI, Dillin A, Kelly JW (2008) Adapting proteostasis for disease intervention. *Science*, 319:916–919.
44. Hernández H, Robinson CV (2007) Determining the stoichiometry and interactions of macromolecular assemblies from mass spectrometry. *Nat Protoc*, 2:715–726.
45. Benesch JLP, Sobott F, Robinson CV (2003) Thermal dissociation of multimeric protein complexes by using nanoelectrospray mass spectrometry. *Anal Chem*, 75:2208–2214.
46. Pace CN, Vajdos F, Fee L, Grimsley G, Gray T (1995) How to measure and predict the molar absorption coefficient of a protein. *Protein Sci*, 4:2411–2423.
47. Fraser GW (2002) The ion detection efficiency of microchannel plates (MCPs). *Int J Mass Spectrom*, 215:13–30.